Low-cost device for ratiometric fluorescence measurements

Yordan Kostov and Govind Rao[a)]
Medical Biotechnology Center and Department of Chemical and Biochemical Engineering, University of Maryland Biotechnology Institute, Baltimore, Maryland 21201

(Received 25 June 1999; accepted for publication 24 August 1999)

An all-solid-state, low-cost device for fluorescent wavelength-ratiometric detection is described. Ultrabright light-emitting diodes were used as light sources. This allowed electronic modulation of the light, simple optical configuration, and miniaturization of the instrument. Narrow-bandpass interference filters were used for wavelength separation. Detection was accomplished by high-sensitivity, large-surface *PIN* photodiodes. An integrating double-ramp technique with fixed upper and lower thresholds was employed for conversion of the light intensities into time intervals. The duty ratio of the output signal was a function of the fluorescence intensity ratio. Additionally, the concentration of the fluorophore could be measured. The device could be easily designed as a battery-operated version. It could be used for a variety of ratiometric fluorescence measurements. © *1999 American Institute of Physics.* [S0034-6748(99)01412-4]

I. INTRODUCTION

Fluorescence wavelength-ratiometric methods have received considerable attention during the last decade. Their main application is in the biomedical field. Ratiometric dyes and combinations of dyes are widely used for measurements of *p*H, Ca^{2+}, Mg^{2+}, Zn^{2+}, heavy metals, and transmembrane potentials.[1–9] This interest is dictated by the possibility of performing measurements without electrical contact with the object under investigation, as well as the possibility for equilibrium measurements.

The ratiometric approach is based on the use of dual-excitation or dual-emission dyes. They possess at least two peaks in their excitation and/or emission spectrum. When in contact with an analyte, the amplitude of one of these peaks is affected—either because of the changes in the electron structure of the dye or because of dynamic quenching. The ratio of the fluorescence intensities at these wavelengths (or at one of the wavelengths and at an isoemissive point) correlates with the concentration of the analyte.

The ratiometric approach offers significant advantages in comparison with conventional steady-state methods. It is well known that the latter are prone to errors due to losses in the optical path, photobleaching, scattering, and background light. This results in the need for very strict experimental conditions and frequent recalibration. Implementation of ratiometry avoids most of these problems.

The standard equipment for the ratiometric measurements is usually a conventional fluorimeter, or a custom-built system.[10] These expensive systems are restricted to laboratory use. In this article, we describe a simple, low-cost device for fluorescence ratioing measurements. It is based on all-solid-state technology. The use of high-brightness light-emitting diodes (LEDs) avoids the need for use of mechanical or other external choppers and permits miniaturization of the device. The high-efficiency semiconductor light sources avoid problems connected with high-power consumption and heat dissipation. The narrow-emission band of these LEDs permitted the use of filters for wavelength selection instead of monochromators. The device could easily be battery operated. It could be used for more accurate ratiometric measurements of fluorescence.

II. DESCRIPTION OF THE INSTRUMENT

A. Optical configuration

The optical configuration of the system was chosen to be as simple as possible, with the intent that it would be used in a low-cost device. The system had to work with solution-phase fluorescent indicators, so the sample compartment was chosen to hold a standard 1 cm disposable cuvette. In this case, the right-angle geometry is superior. In the case of nonturbid solutions it allows an increased signal-to-noise ratio (SNR).

LEDs are the natural choice for light emitters in low-cost devices. At present, there are commercially available LEDs, which cover the whole visible region[11] and part of the UV.[12] The LEDs used in the device were chosen to match the excitation maxima of the indicator dye as closely as possible.

The number of the emitters and detectors in the scheme depends on the type of the indicator employed. For characterization of the device, a dual-excitation indicator was used. It was *p*H-sensitive carboxydichlorofluorescein, in solution. The optical path is shown in Fig. 1.

The dual-excitation indicator required two light sources. They were a high-brightness, blue LED MBB51TAH-T (Micro Electronics Corp., Santa Clara, CA), maximum wavelength 470 nm, 40 nm full width at half maximum (FWHM), luminous intensity 4000 mcd, and a green NSPG 500 (Nichia, Mounville, PA), maximum wavelength 520 nm, 40 nm FWHM, luminous intensity 5000 mcd. The output light was filtered using narrow-bandpass interference filters: 470 ± 10 and 520 ± 10 nm. The emission filter was 590 ± 40 nm. The

a)Author to whom all correspondence should be addressed; electronic mail: grao@umbc.edu

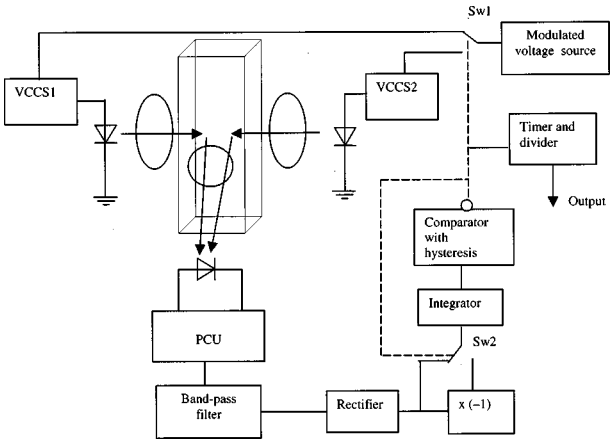

FIG. 1. Optical configuration for dual-excitation fluorescence measurements and electronical diagram of the device. Abbreviations: VCCS, voltage-controlled current source; PCU, photoconversion unit; and Sw, switch.

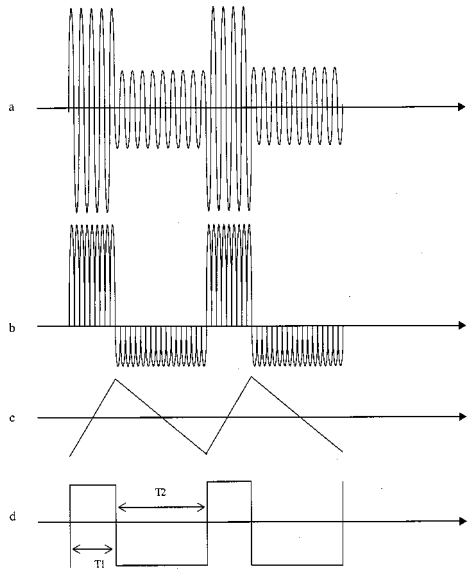

FIG. 2. Time diagrams of the signals. See the text for details.

transmission of the excitation filters in the passband was 50%, and the transmission of the emission filter was 75%. The absorption of the filters in the stop band was greater than 4. All the filters were from Intor, Inc. (Sorocco, NM). The fluorescence was collected using a large active area (13 mm^2) *PIN* photodiode S1223-01 (Hamamatsu, Bridgewater, NJ). The filters, LEDs, and the photodiodes were mounted as close as possible to the cuvette, forming a rigid optical unit with the shortest possible light path.

B. Electronic arrangement and principle of operation

The LEDs were driven using custom-built voltage-controlled current sources with shutdown. In the dual-excitation mode, only one LED was working at a time. The LED current was modulated at frequency $f_{\mathrm{mod}}=3$ kHz. The LEDs were operated in pulsed mode (rectangular square wave with 50% duty ratio) at a peak current of 60 mA—twice as much as the nominal rating. The total output optical power from the blue LED was approximately 3.3 mW, and the power from the green was approximately 1.4 mW.

The detection and conditioning electronics are shown in Fig. 1. They consist of a photoconversion unit, filter, rectifier, multiplier by (-1), integrator, and comparator with hysteresis.

When one of LEDs emits modulated light, the other is off. The light from the working LED passes through an excitation optical filter and excites fluorescence in the sample cuvette. The fluorescence passes through an emission optical filter. It is detected by a photoconversion unit, which consists of a photodiode, transimpedance amplifier, and an appropriate second amplification stage. This signal is passed through a second-order, narrow-bandpass ($Q=10$) active Chebyshev filter with unity gain. The center frequency is chosen to be equal to the modulation frequency of the LED. The bandpass filter rejects steady-state components, which originate from the ambient light, and diminishes the level of the low- and high-frequency noise. The amplitude of the resulting ac is determined by passing it through a rectifier. However, in order to be able to distinguish between signals that originate from the different wavelengths, a sign is assigned to the rectified signals, so on the input of the integrator the signals from the both wavelengths always have opposite signs. The output from the bandpass filter and input signals on the integrator are shown in Figs. 2(a) and 2(b). The output of the integrator is connected to a trigger with hysteresis, which controls switches Sw1 and Sw2.

If the input signal of the integrator is positive, this will cause a gradual increase of the voltage on the integrator output [Fig. 2(c)]. When it reaches the upper threshold of the hysteresis trigger, the output switches to the opposite condition [Fig. 2(d)], changing the positions of switches Sw1 and Sw2. Now the signal from the other investigated wavelength (from the second LED) is fed into the integrator, but it has an opposite sign. This causes the gradual decrease of the integrator's output voltage. When it reaches the lower threshold of the hysteresis trigger, it switches back, and the process is repeated. As a result, a square wave appears on the output of the trigger.

The current that flows through the integrator during the time interval, equal to a half period of the modulating frequency, is given by the following equations:

$$I_i=\int_0^{1/2f} I_{F1}\sin 2\pi f t dt, \quad I_2=-\int_0^{1/2f} I_{F2}\sin 2\pi f t dt, \qquad (1)$$

or

$$I_i=\frac{2}{\pi}I_{F1}, \quad I_2=-\frac{2}{\pi}I_{F2}, \qquad (2)$$

respectively. Here, f denotes the modulation frequency of the excitation light, and I_{F1} and I_{F2} are the amplitudes of the fluorescence signals corresponding to each wavelength of interrogation. The signal is harmonic, as the high-frequency components of the rectangular LED modulation are suppressed by the bandpass filter. The output voltage of the integrator is proportional to the integral of the current flowing through the capacitor. If the initial and final voltages are

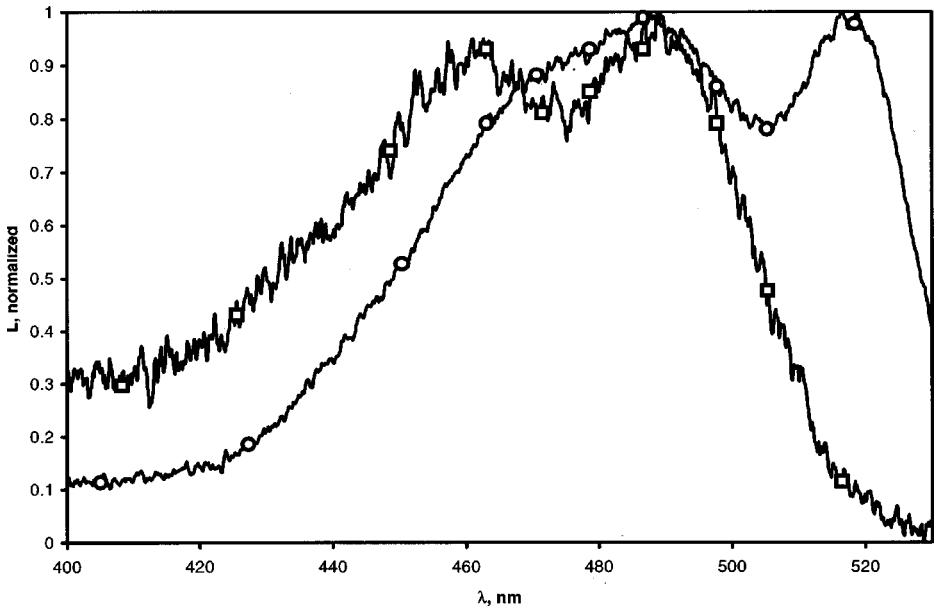

FIG. 3. Fluorescence excitation spectra of 5-(and 6-) CDCF, mixed isomers. (□), *p*H 2.55 and (○), *p*H 9.30.

the lower U_{lo} and the upper U_{up} threshold of the trigger, then the integration times T_1 and T_2 will be given by the equations

$$T_1=\frac{\mathrm{RC}(U_{up}-U_{lo})}{n_1 I_1}, \quad T_2=\frac{\mathrm{RC}(U_{up}-U_{lo})}{n_2 I_2}. \tag{3}$$

Here, RC is the integration constant. In Eqs. (3) and (4) the time intervals are assumed to be equal to a whole number of half waves; as the length of the integration time is usually more than 10^3 times longer than the length of one half wave, this does not introduce significant error. Now, if the ratio of the intensities is calculated by

$$\frac{I_{E1}}{I_{E2}}=K\frac{T_2}{T_1}, \tag{4}$$

the ratio of the time intervals (T_2/T_1) is proportional to the luminescence intensity ratio. The period of the square wave (T_1+T_2) is proportional to the concentration of the fluorophore. The ratio of the time intervals is evaluated either using a timer (digitizing the lengths of the intervals) and numerical calculation of the ratio, or simply by measurement of the dc component [duty ratio (DR)] of the square wave. As $\mathrm{DR}=T_1/(T_1+T_2)$, the ratio is given by the equation

$$\frac{T_2}{T_1}=\frac{1}{\mathrm{DR}-1}. \tag{5}$$

C. Error considerations

The biggest source of error was the noise from the photodiode. All other possible sources of noise (like the switching noise of the multiplexer, etc.) were smaller by an order of magnitude, as measured in the setup.

The noise contributes to error in the time intervals T_1

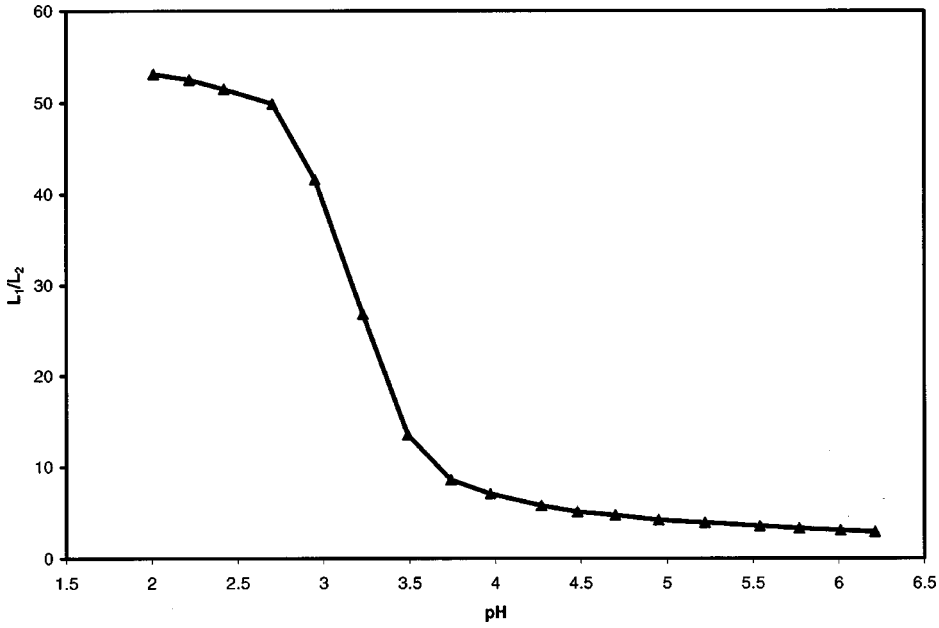

FIG. 4. Calibration curve of the radiometric device for 5-(and 6-) CDCF.

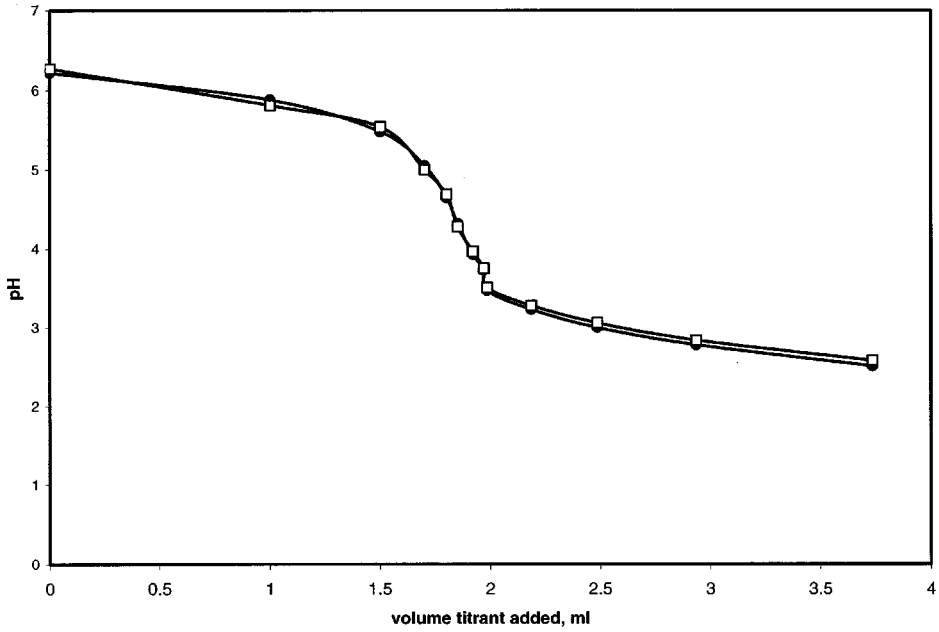

FIG. 5. Comparison between the *p*H, measurements as determined by the device, and a conventional *p*H meter. (●), Orion 230 A and (□), device.

and T_2. Hence, the standard deviation of the measurement could be described as

$$\sigma^2=\frac{\sigma_{T_1}^2}{T_1^2}+\frac{\sigma_{T_2}^2}{T_2^2}=\frac{1}{\mathrm{RC}\Delta U}\left(\frac{\sigma_{T_1}^2}{n_1^2I_{E1}^2}+\frac{\sigma_{T_2}^2}{n_2^2I_{E2}^2}\right). \tag{6}$$

Consequently, the error in the measurement could be diminished using two independent approaches—increasing the integration constant RC or increasing the difference between the thresholds of the hysteresis trigger.

III. PERFORMANCE AND DISCUSSION

The use of semiconductor light sources greatly simplified the optics of the device. The small dimensions and the negligible power dissipation of the LEDs made it possible to place them in close proximity to the sample compartment. This minimized the light path and allowed the excitation light to be efficiently coupled into the sample without the use of focusing optics. The total optical power, coupled into the sample, was 406 μW at 470 nm, and 67 μW at 520 nm.

The use of LEDs also allowed electronic modulation of the excitation light intensity at relatively high frequency, 3 kHz. The frequency was chosen to be much higher than the ever-present 60 Hz, but still far before the roll-off of the transimpedance amplifier.

The narrow emission of the LED allowed the use of narrow-bandpass interference filters instead of monochromators in the excitation paths. However, the emission filter was selected to be wide-bandpass, with the same rejection ratio outside the band ($A \geqslant 4$), to measure greater fluorescence signals and to improve the SNR.

The device was used for detection of *p*H using ratiometric dye. It was 5-(and 6-)-carboxy-2′7′-dichlorofluorescein, mixed isomers (Molecular Probes, Inc., Eugene, OR) [5-(and 6-CDCF)], pKa 3.8. Its fluorescence excitation spectra are shown in Fig. 3. This is a dual-excitation indicator. As can

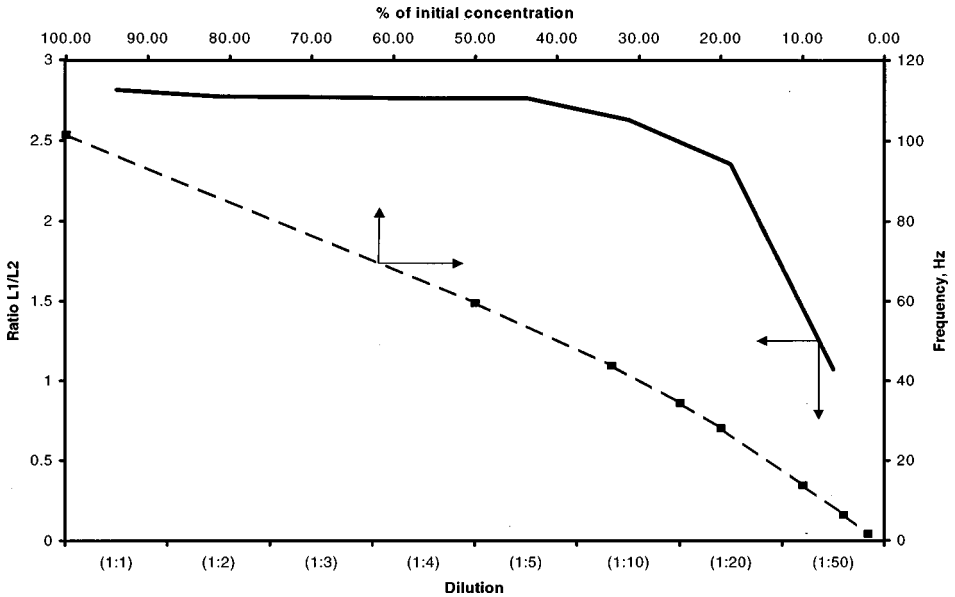

FIG. 6. Dependence of ratio L_1/L_2 and output frequency on dilutions. Upper curve, ratio L_1/L_2 vs dilutions and lower curve, the frequency vs indicator concentration.

be seen, both acidic and basic forms of the indicator possess an excitation maximum at 482 nm. The basic form of the indicator also possesses a well-defined excitation peak at 518 nm, while the acidic form almost does not fluoresce when excited at this wavelength. Thus, the ratio of the emission intensities above 550 nm (when the indicator is excited at 470 ± 10 and 520 ± 10 nm) strongly depends on the *p*H of the solution. The indicator concentration used was 2 μmol/l, which was the initial concentration for the dilution tests. The right-angle geometry and configuration for dual excitation were used.

The performance of the device was evaluated in two steps: (a) determination of the calibration curve of the device and (b) comparison of *p*H determined by the device and a commercial *p*H meter—model 230 A (Orion). In both cases the initial solution contained 2 μmol/l 5-(and 6-)CDCF in 0.1 M phosphate buffer with *p*H 6. It was titrated with 0.1 M HCl, to which 2 μmol/I 5-(and 6-)CDCF was added. The calibration curve is shown in Fig. 4. Figure 5 shows the comparison between *p*H determined by the device and the standard *p*H meter. Almost in the whole range the *p*H could be determined with accuracy of 0.05 *p*H units. The errors, as expected, were smallest in the region around the pK_a of the dye. At both ends of the calibration curve the errors were higher. The highest error ($\Delta=0.08\,p$H) was in the most acidic point of the range. This could be explained by the fact that at very low *p*H the indicator has negligible fluorescence when excited at 520 nm. This strongly degrades the SNR and introduces some offset in the measured values.

As mentioned previously, the ratiometric measurements should be relatively independent of the changes in the dye concentration (due to different preparations, photobleaching, etc.). In order to confirm that, several different concentrations of the dye were prepared at the same *p*H (5.0), and the response of the device to the samples was measured. As can be seen from Fig. 6, the measured output of the sensor was almost independent of the concentration up to dilutions of 20:1. At higher dilutions, the noise on the input of the photodetector begins to prevail.

In the case when higher independence from the indicator concentrations is needed, or when samples with lower concentration should be measured, several steps can be taken to improve the SNR. First of all, shielding of the photodetector would greatly diminish the noise; the use of higher-order Chebyshev bandpass filters will also diminish the noise bandwidth. Additional improvements could be achieved if synchronous detection of the signal is used, together with longer integration times. However, even this simple version of the device showed good immunity to noise.

During long-term experiments it is desirable to follow the concentration of the indicator in order to detect when the dye is photobleached to the extent that it should be changed. As the sum of the time intervals, $T1+T2$ (and hence, the frequency at the trigger's output) is proportional to the concentration of the dye, it could be used as a parameter indicating the need for change of the sensing dye. In Fig. 6 the dotted curve represents the experimentally measured frequency when the sample is diluted. It was proportional (within the experimental error) to the concentration of the indicator.

Another possible source of error in the fluorescence measurements is scattering of the excitation light in the media. Although the filters used have quite high absorption in the stop band, scattered excitation light could be comparable with the fluorescence intensity. In order to evaluate the influence of the scattering on the setup, the device was tested with two samples of 5-(and 6-) CDCF at *p*H 3.8, one of which contained 0.5% of colloidal silica (Ludox HS30, DuPont, Wilmington, DE) added as a scatterer. The difference in the output ratio was less than 1%.

With minor changes (using one LED for excitation and two photodetectors), the device could be used for dual-emission indicators. Another possible application is the use of indicators immobilized in sensing membranes. However, the latter would require changes in the optical configuration—the low thickness of the membranes imposes a requirement for front-face geometry.

In conclusion, the presented ratioing device has been shown to operate successfully under various experimental conditions. The device is all-solid state, rugged, and low cost. Its low-power consumption allows it to be adapted easily to battery operation.

ACKNOWLEDGMENTS

The authors thank the referee for the helpful suggestions. One of the authors (Y.K.) thanks Peter Harms for many helpful discussions and extensive reading of the manuscript. This work was supported by funds from NIH (Grant Nos. RR-10955 and RR-14170) and unrestricted funds from Genentech, Merck, and Pfizer.

[1] M. Nedergaard, S. Desai, and W. Pulsinelli, Anal. Biochem. **187**, 109 (1990).
[2] B. S. Gan, E. Krump, and S. Grinstein, Am. J. Physiol. **275**, 1158 (1998).
[3] I. C. Spencer and J. R. Berlin, Pflugers Arch. Ges. Physiol. Menschen Tiere **430**, 579 (1995).
[4] M. Yassine, J.-M. Salmon, and P. Viallet, J. Photochem. Photobiol., B **37**, 18 (1997).
[5] A. Salvi, J. M. Mayer, P. A. Carrupt, and B. Testa, J. Pharm. Biomed. Anal. **15**, 149 (1996).
[6] B. L. Sabatini and W. G. Regehr, Biophys. J. **74**, 1549 (1998).
[7] K. Meuwis, N. Baens, and M. Vincent, Chem. Phys. Lett. **287**, 412 (1998).
[8] L. M. Loew, Pure Appl. Chem. **68**, 1405 (1996).
[9] R. P. Haugland, *Handbook of Fluorescent Probes and Research Chemicals*, 6th ed. (Molecular Probes, 1996).
[10] Z. Xu, A. Rollins, R. Alcala, and R. E. Marchant, J. Biomed. Mater. Res. **39**, 9 (1998).
[11] P. Harms, J. Sipior, N. Ram, G. M. Carter, and G. Rao, Rev. Sci. Instrum. **70**, 1535 (1999).
[12] High Power Can Type UV LED NSHU 550E, Nichia product guide, Nichia Chemical Industries.